Supporting Information

Anisotropic Bacterial Cellulose Hydrogels with Tunable High Mechanical Performances, Non-Swelling and Bionic Nanofluidic Ion Transmission Behavior

Minghao Zhang, Shiyan Chen*, Nan Sheng, Baoxiu Wang, Zhuotong Wu, Qianqian Liang, Huaping Wang*

State Key Laboratory for Modification of Chemical Fibers and Polymer Materials, College of Materials Science and Engineering, Donghua University, Shanghai 201620, PR China
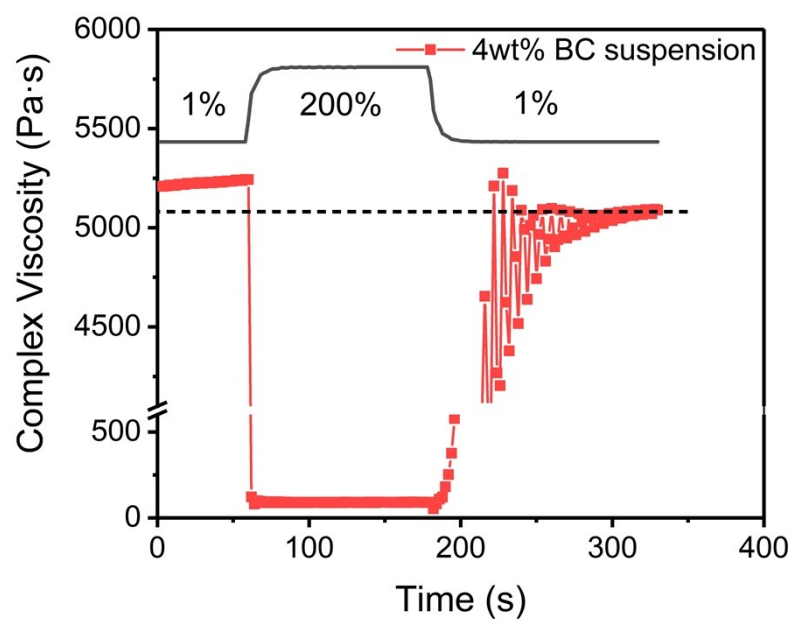
Email addresses: chensy@dhu.edu.cn; wanghp@dhu.edu.cn

Fig. S1. Dynamic rheological three-interval time test of 4% BC suspension with 15% urea content showing its thixotropy.

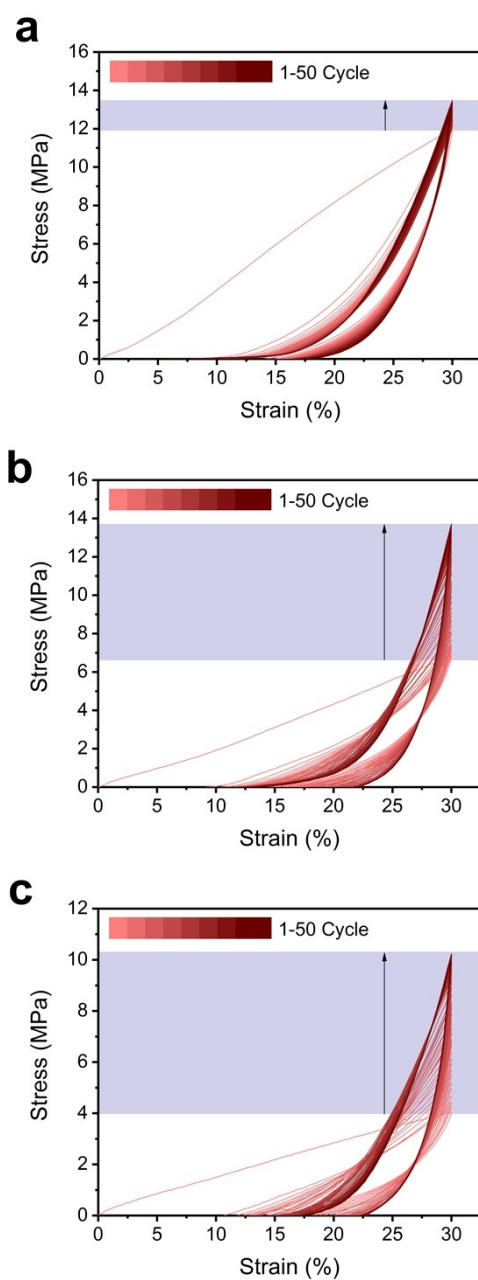**Fig. S2.** The photograph of ABCH-15-0 and ABCH-15-5.0.

Fig. S3. Representative tensile stress–strain curves of ABCH-10-3.0 (a), ABCH-20-7.0 (b), and ABCH-25-7.0 (c) during loading–unloading cycles of fixed strains.

The ABCHs with fewer nanofibers will have lager residual strain. The increases in maximum tensile stress during cycling demonstrated that the rigid nanofiber network will promote the recovery of the deformation of ABCHs.
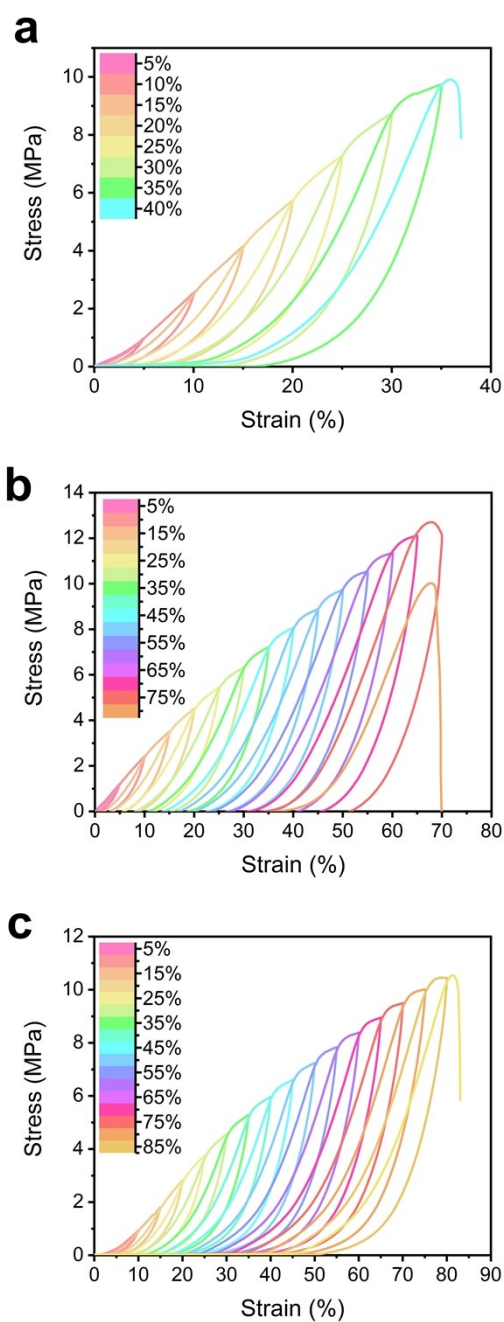
Fig. S4. Representative tensile stress–strain curves of ABCH-10-3.0 (a), ABCH-20-7.0 (b), and ABCH-25-7.0 (c) during loading–unloading cycles of varying strains. Taking the highest point of the previous cycle as the reference point, the front part of the second loading curves is J-shaped and transforms S-shaped later. The ABCHs with fewer nanofibers will have a more obvious change of shape between the two segments of the curve.
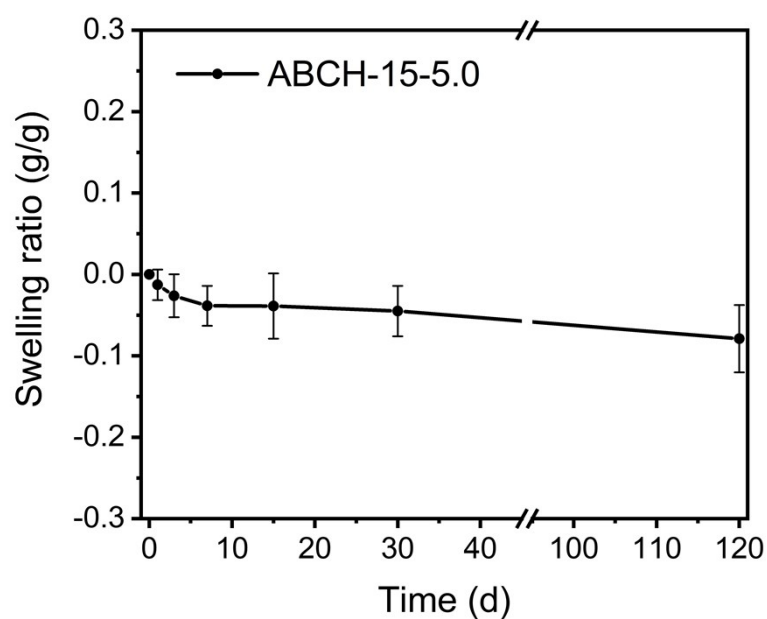
Fig. S5. Swelling ratio (g/g) curve of ABCH-15-5.0. The equilibrium swelling rate of ABCH hydrogels does not increase after soaking in water for 120 days. Minor quality loss may come from the degradation of the hydrogels.
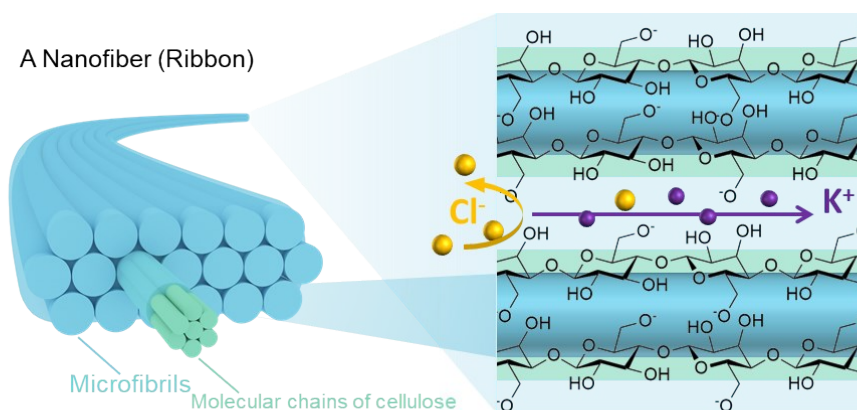

Fig. S6. Schematic diagram of nanochannels with negative surface charge in nanofibers.
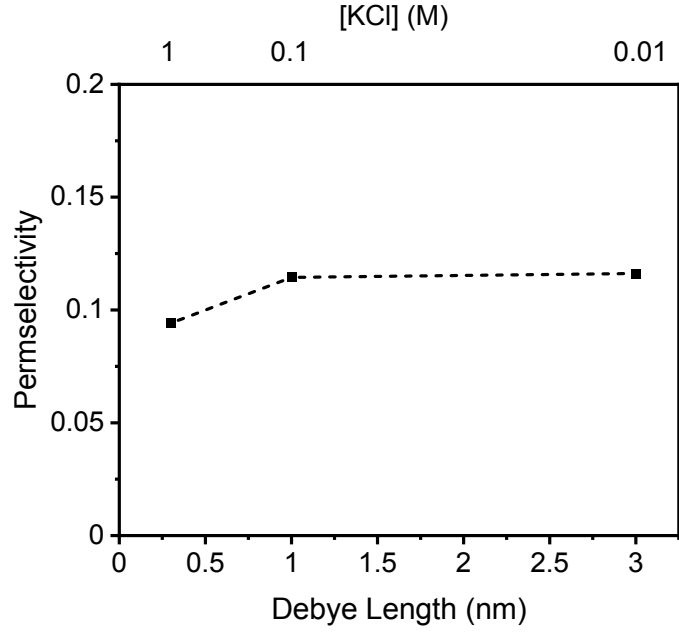
Fig. S7. The measured permselectivity values were plotted as a function of the Debye length and KCl concentration.

The static current generated by ion selectivity will cause the generation of voltage, so the ion selectivity can be quantified by measuring the open-circuit voltage. We varied the KCl concentration in one of the sides while leaving the concentration in the other side constant. The cation transference number (t^+) calculated by equation (S1) [1] represents the index of cation selectivity, which equals 1 for ideal cation selective case and equals 0 for ideal anion selective case:

$$t^+ = \frac{1}{2}\left(\frac{E_{diff}}{\frac{RT}{zF}\ln\left(\frac{\gamma_H c_H}{\gamma_L c_L}\right)} + 1 \right) \quad (S1)$$

where R, T, z, F, γ, c represent the gas constant, temperature, charge valent, Faraday constant, activity coefficient of ions, ion concentrations, respectively.

The permselectivity (P) was then calculated by equation (S2) using the cation transport number in bulk ($t^+_{bulk} = 0.49$ for KCl solution):

$$P = \frac{t^+ - t^+_{bulk}}{1 - t^+_{bulk}} \quad (S2)$$

As shown in Fig. S7, for ABCH-15-5.0, the t^+ of each concentration is about 0.55 with the permselectivity of about 0.11, which indicates the existence of anion selectivity. And it decreases as the salt concentration increases.
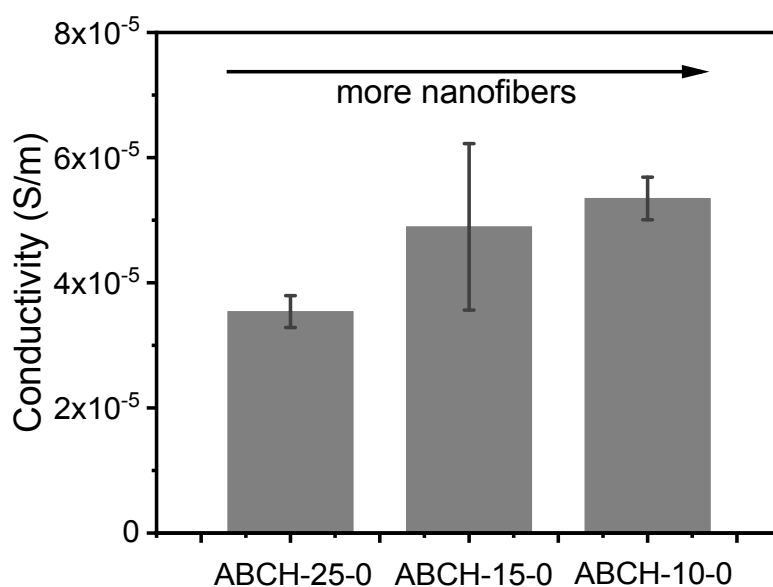

Fig. S8. Ionic conductivity of ABCH-10-0, ABCH-15-0 and ABCH-25-0 in 10^{-6} M KCl solution.

The higher conductivity of ABCH with more nanofibers indicates the positive effect of more nanofibers on the conductivity of the hydrogel.

Theory for the quantification of ionic conductivity of the macro hydrogel nanofluid device

The nanofluid spaces between the microfibrils in BC nanofibers are considered to be negatively charged nanochannels, and a constant ion mobility and a constant net surface charge are assumed. The conductance G [S] of a single nanochannel in nanofibers for all KCl concentrations can be described as the superimposition of the bulk conductance and the excess counterion conductance [2]:

$$G = 10^{-3} z (\mu_+ + \mu_-) c N_A e \frac{wh}{d} + 2\sigma_s u_+ \frac{w}{d} \quad (S3)$$

where Z is the cation valence, μ_+ and μ_- [m^2 V^{-1} s^{-1}] is the mobility of the cation (K$^+$) and anion (Cl$^-$), respectively, c [M=mol L^{-1}] is the concentration of ion, N_A [mol^{-1}] is the Avogadro constant, and e [C] is the electron charge, w [m], h [m] and d [m] are the width, height and length of the nanochannel, σ_s [C m^{-2}] is the effective surface charge density.

According to the relationship between conductance and conductivity:

$$\sigma = \frac{Gd}{wh} \quad (S4)$$

The conductivity of a single channel can be expressed as:

$$\sigma = 10^{-3} z (\mu_+ + \mu_-) c N_A e + \frac{2\mu_+ \sigma_s}{h} \quad (S5)$$
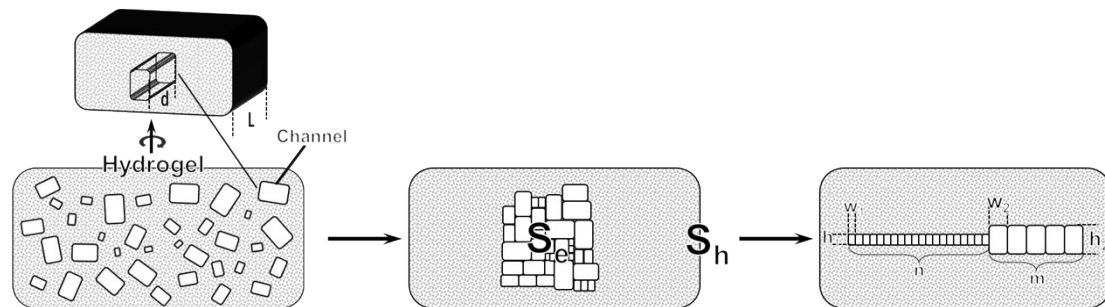

Fig. S9. From left to right: Schematic diagram of the hydrogel model with ideally

channels (d = L); Schematic diagram of the effective area of the channel in the model; Schematic of the simplified model with uniform nanochannels and mesochannels.

Below, we first provide a simplified model to demonstrate the interrelationship of conductance between the hydrogel and a single channel in the nanofiber. In this model, a thin slice of hydrogel cut along the cross section is regarded as composed of the channel running through it (length **d** of channels equal to length **L** of hydrogel) for ions transmission as well as the substance that prevents ions from passing (Fig. S9). So the effective area of ion channels (s_e) can be expressed as:

$$s_e = \alpha s_h \ (0 < \alpha < 1) \ (S6)$$

where S_h is the measured cross-sectional area of the hydrogel, α is the ratio of the effective area to the cross-sectional area of the hydrogel.

Then, due to the conductance of the hydrogel (G_h) actually equivalent to the effective conductance from channels (G_e), the effective conductivity of the channels (σ_e) can be expressed as:

$$\sigma_e = \frac{G_e d}{s_e} = \frac{G_h L}{s_e} = \frac{1}{\alpha}\sigma_h \ (S7)$$

The effective area of the nanochannel can be seen as completely filled with KCl solution, and σ_e should be similar to the conductivity of the KCl bulk at high concentrations. So $\alpha = 0.0597$ can be calculated using equation (S7), where the approximate value of σ_e obtained by $\sigma_{KCL \ bulk}$ under 1M concentration and σ_h obtained by measurement. Then the effective conductivity σ_e at different concentrations can be obtained and plotted in **Fig. S10.**
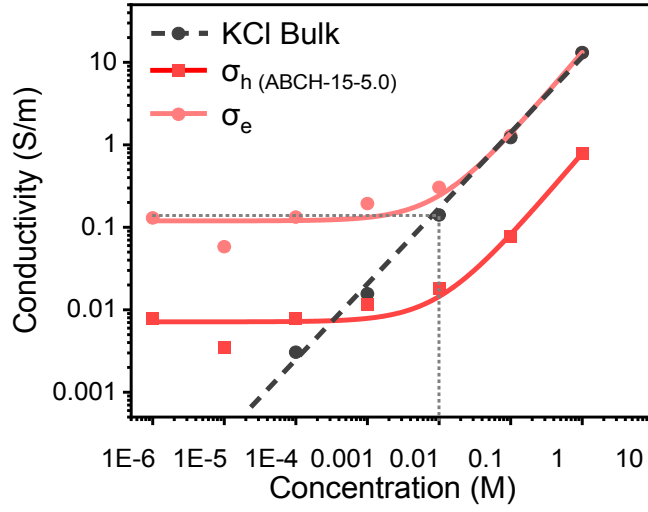
Fig. S10. The curve of conductivity of the hydrogel (σ_h) and the calculated effective conductivity of the channels (σ_e).

From equation S5, the effective conductivity of channels (σ_e) can be expressed as:

$$\sigma_e = 10^{-3}z(\mu_+ + \mu_-)cN_A e + \frac{2\mu_+ \sigma_s}{h} \quad (S8)$$

The surface charge density (σ_s) can be obtained according to equation S9 [3]:

$$\sigma_s = \frac{\varepsilon\varepsilon_0\zeta}{\lambda_d} \quad (S9)$$

where ε is the dielectric constant of pure water, ε_0 is the permittivity of vacuum, $\zeta [mV]$ is the zeta potential. The Debye length λ_d [m] in electrolyte solution can be express as S10 [4]:

$$\frac{1}{\lambda_d} \sim \sqrt{\lambda_B I} = \sqrt{\frac{e^2}{\varepsilon\varepsilon_0 K_B T}\sum_i c_i Z_i^2} \quad (S10)$$

Where e [C] is the elementary charge, K_B [J m^{-1}]is the Boltzmann constant, T is the temperature [K], λ_B [m] is Bjerrum length.

According to equation (S8-10), the Debye length is about 3 nm in a concentration of

0.01 M KCl solution, the channel height **h** inside the hydrogel can be calculated to be about 1.4 nm, and the surface charge density of hydrogel are calculated to be 1.5 mC m^{-2} at this time.

In fact, in addition to the nanochannels, there are also many mesochannels in hydrogel. The height of these channels is much greater than the Debye length even at low concentrations, so the conductivity through these channels is also determined by the bulk conductivity of the ionic solution.

We further simplified the hydrogel model to have nanochannels and mesochannels with uniform sizes, respectively (Fig. S9). The effective area of all of the channels can be expressed as:

$$S_e = nw_1h_1 + mw_2h_2 \quad (S11)$$

where n, w_1 [m] and h_1 [m] are the number, width and height of the nanochannels; m, w_2 [m] and h_2 [m] are the number, width and height of the mesochannels.

Then, W_1 and W_2 were used to refer to nw_1 and nw_2 respectively for further simplify equation, σ_e can be expressed as:

$$\sigma_e = 10^{-3}z(\mu_+ + \mu_-)cN_Ae + 2\mu_+\sigma_s\left(\frac{W_1 + W_2}{W_1h_1 + W_2h_2}\right) \quad (S12)$$

where $W_1 \gg W_2$ and $h_1 \ll h_2$, in other words, that means the mesochannels do not contribute to the increase of the conductivity plateau value at low concentration, so the equation (S12) can be simplified to:

$$\sigma_e = 10^{-3}z(\mu_+ + \mu_-)cN_Ae + 2\mu_+\sigma_s\left(\frac{W_1}{W_1h_1 + W_2h_2}\right) \quad (S13)$$

Assuming that β is the ratio of the area occupied by the nanochannels to the total effective area, then:

$$\beta = \frac{W_1 h_1}{W_1 h_1 + W_2 h_2} = 1 - \frac{W_2 h_2}{W_1 h_1 + W_2 h_2} \quad (S14)$$

And σ_e can be futher expressed as:

$$\sigma_e = 10^{-3} z (\mu_+ + \mu_-) c N_A e + 2\mu_+ \sigma_s \left(\frac{\beta}{h_1}\right) \quad (S15)$$

And σ_h can be further expressed as:

$$\sigma_h = \alpha [10^{-3} z (\mu_+ + \mu_-) c N_A e + 2\mu_+ \sigma_s \left(\frac{\beta}{h_1}\right)] \quad (S16)$$

Where α and β could be seen as a correction factor to express the conductivity of macro hydrogel more accurately.

When the number of nanofibers in the hydrogel increases, the conductivity of the hydrogel will increase due to the increase value of W_1 followed by the increase of β, which is consistent with our measured results in Fig. S8.

At same times, using equations (S8 and S15), we can find the relationship of h and h_1 to enable the height of the nanopore to be more accurately estimated:

$$h_1 = (1 - \beta)h \quad (0 < \beta < 1) \quad (S17)$$

It can be seen that the actual size of the nanochannels should be smaller than the h previously calculated (less than 1.4nm) based on the equations (S8).
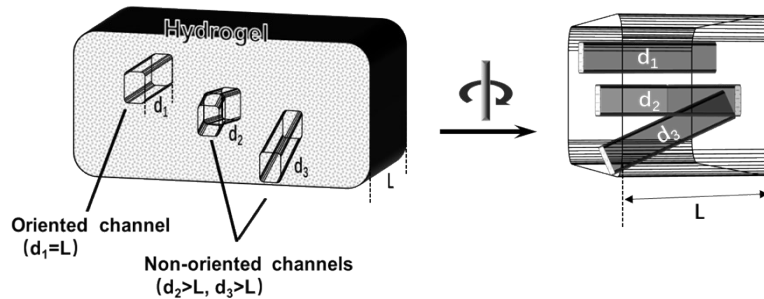

Fig. S11. Schematic diagram of ideal channels in oriented nanofibers (d=L) and in non-oriented nanofibers (d<L).

Further, if the nanofibers are not well oriented in the hydrogel, it will not be suitable for the ideal model we described above. At this time, we can assume that the length of the channel (d) is larger than that of the hydrogel (L) instead of equal (Fig. S11). According to equations (S7, S8), the conductivity of the hydrogel (σ_h) can be expressed as:

$$\sigma_h = \frac{G_h L}{s_h} = \alpha[10^{-3}z(\mu_+ + \mu_-)cN_A \mathcal{e} + 2\mu_+ \sigma_s\left(\frac{\beta}{h_1}\right)]\frac{L}{d} \quad (S17)$$

When the nanochannels are not effectively oriented, the conductivity of the hydrogel will decrease due to d>L, which is consistent with our measured results in Fig. 4b.
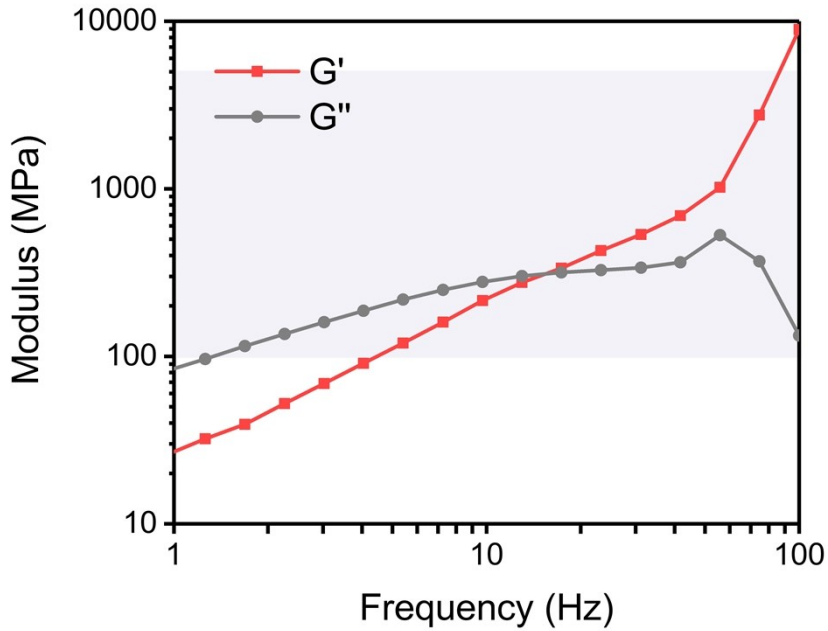

Fig. S12. Oscillation shear frequency sweep of 0.5 wt% agar with constant strain amplitude as 7%. The purple shaded area represents the range of nerve tissue shear modulus.
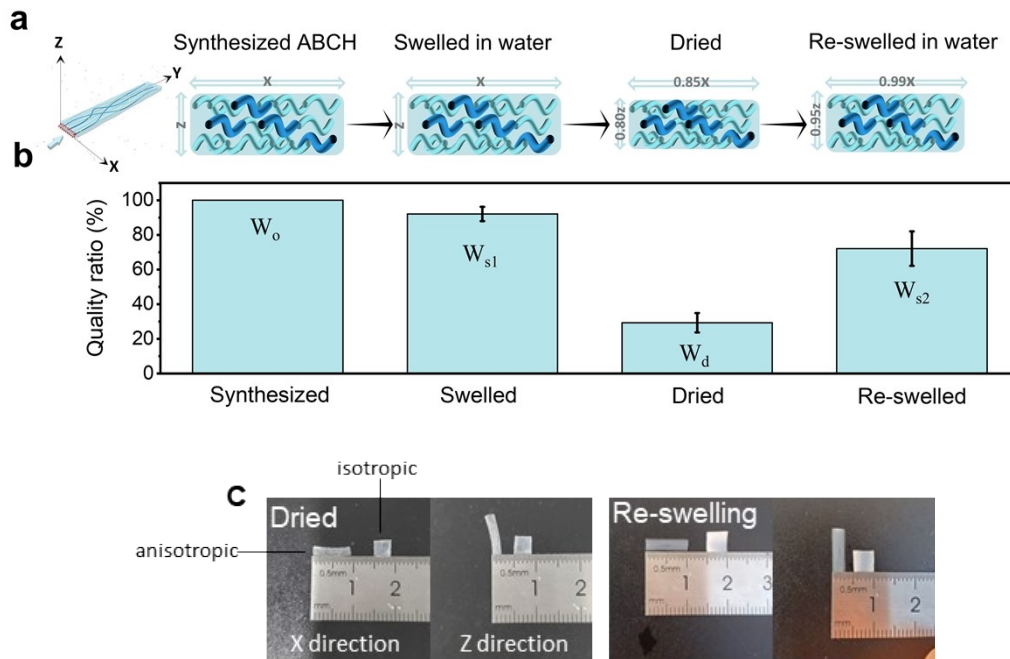
Fig. S13. (a) ABCHs have limited volume change in radial direction after complete dehydration. Thereby, they will also have limited volume change when they continue to swell when immersed in pure water. (b) Quality change of ABCH-15-5.0 after swelled, dried and re-swelled. (c) The photograph of anisotropic and isotropic hydrogels before and after re-swelling.

The ABCHs show similar swelling properties along X-direction and Z-direction, while the unmarked Y-direction re-swelling is not obvious. For our isotropic hydrogel, its swelling behavior is also isotropic.
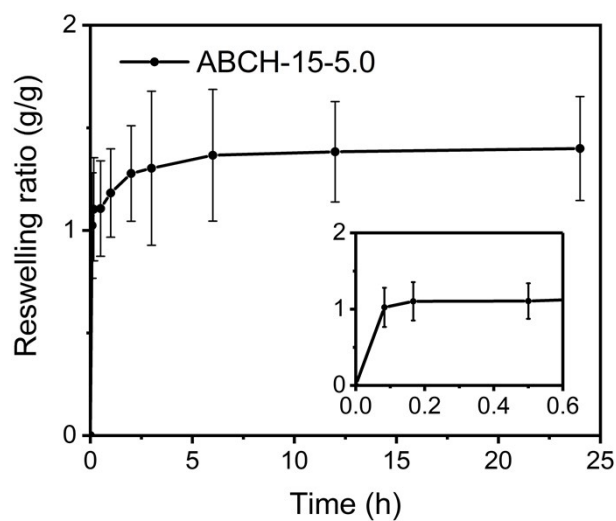

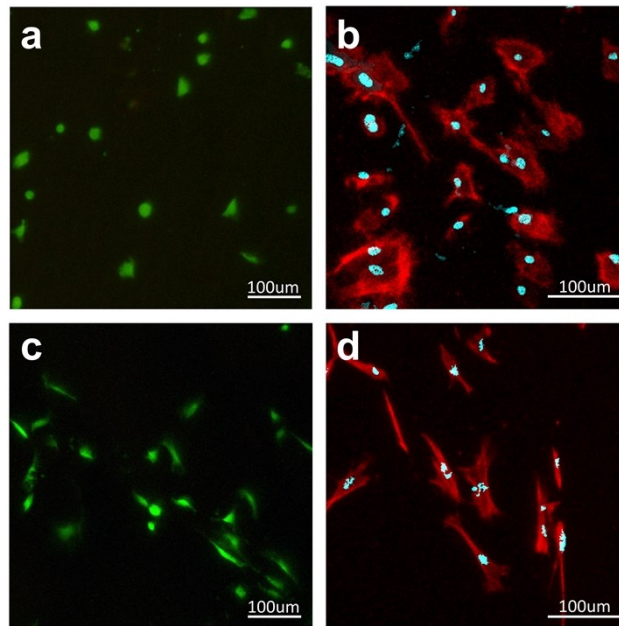**Fig. S14.** Reswelling ratio (g/g) curve of ABCH-15-5.0 over time.

Fig. S15. Laser confocal images of cell viability (a, c) and (b, d) morphology on the surface of ABCH-15-0 (a, b) and ABCH-15-5.0 (c, d) after culturing for 3 days. Compared with the relatively round cells on ABCH-15-0, the cells on ABCH-15-5.0 show a fusiform morphology and tend to be aligned along the direction of nanofibers in the hydrogels.
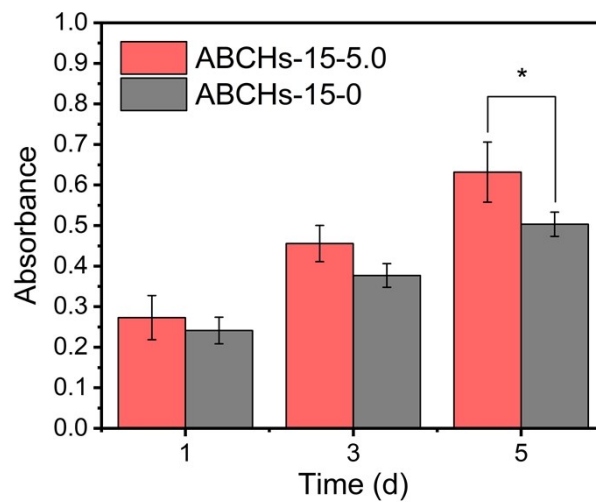

Fig. S16. Cell proliferation of MSCs on the surface of ABCH-15-0 and ABCH-15-5.0 at days 1, 3 and 5. Aligned nanofibers in ABCH-15-5.0 can boost cell proliferation to a certain extent.

Table S1 Mechanical properties and water content of ABCHs with different urea content.

Sample	Strength (MPa)	Modulus (MPa)	Water content (%)
ABCH-10-3.0	13.1±1.6	47.4±6.9	70.6±4.4
ABCH-15-5.0	14.3±2.2	38.9±11.2	70.7±5.6
ABCH-20-7.0	12.6±1.8	26.9±3.8	67.3±1.8
ABCH-25-7.0	9.8±2.0	15.6±3.2	69.6±1.2

Table S2 Mechanical properties and water content of ABCHs with different DR values.

Sample	Strength (MPa)	Modulus (MPa)	Water content (%)
ABCH-15-0	4.8±1.1	2.7±0.8	85.4±4.7
ABCH-15-1.0	6.3±2.3	3.8±0.2	80.7±2.6
ABCH-15-3.0	8.3±0.5	11.0±2.2	72.5±1.8
ABCH-15-5.0	14.3±2.1	38.9±11.2	70.7±5.6

Reference

1.   Y.-C. Yao, A. Taqieddin, M. A. Alibakhshi, M. Wanunu, N. R. Aluru and A. Noy, *ACS Nano*, 2019, **13**, 12851-12859.

2.   C. Yang and Z. Suo, *Nat. Rev. Mater.*, 2018, **3**, 125-142.

3.   H.-R. Lee, C.-C. Kim and J.-Y. Sun, *Adv. Mater.*, 2018, **30**, 1704403.

4.   J. P. Thiruraman, P. Masih Das and M. Drndić, *ACS Nano*, 2020, **14**, 3736-3746.